THE GEOMETRIC FILTERING EFFECT ON RIDE COMFORT OF THE RAILWAY VEHICLES

Dragoș Ionuț STĂNICĂ[1], Mădălina DUMITRIU[2], Mihai LEU[3]

The geometric filtering effect of the excitations derived from the vertical track irregularities is an important feature of the behaviour of vibrations of the railway vehicle. The paper herein examines the influence of this effect upon the ride comfort, by using results from numerical simulations. The numerical simulation applications are developed on the basis of a rigid-flexible coupled vehicle model type, where the bogies and wheelsets are represented by rigid bodies and a 'flexible carbody' model is used for the carbody. The efficiency of the geometric filtering effect is determined on the basis of the velocity range covered by the geometric filtering velocities, at the resonant frequencies of the carbody vibration modes, relevant for the ride comfort. The results show that the ride comfort does not continually deteriorate due to the geometric filtering effect; this effect is efficient on a larger velocity range in the case of rigid carbodies.

Keywords: railway vehicle, geometric filtering effect, vibration, ride comfort

1. Introduction

The railway vehicle is a complex oscillating system, which exhibits vibrations behaviour with specific characteristics [1, 2]. The railway vehicle vibrations develop both in the vertical and horizontal plane, in the shape of translation and rotation moves, independent or coupled among them. The construction of the railway vehicle usually comply with the rules of geometric symmetry, inertial and elastic, hence the moves in the vertical plane can be regarded as decoupled from the ones in the horizontal plane and, for that reason, separately dealt with [3, 4].

An important feature of the behaviour of vertical vibrations of the railway vehicles is the geometric filtering effect of the excitations coming from the vertical track irregularities. This effect exclusively depends on how the track-generated excitations are conveyed to the suspended masses of the vehicle through the wheelsets, irrespective of the suspension characteristics.

[1] PhD student, Doctoral School of Transports, University POLITEHNICA of Bucharest, Romania, e-mail: dragosionutstanica@yahoo.com
[2] Prof., Department of Railway Vehicles, University POLITEHNICA of Bucharest, Romania, e-mail: madalinadumitriu@yahoo.com
[3] PhD student, Doctoral School of Transports, University POLITEHNICA of Bucharest, Romania, e-mail: mihaileu.c@gmail.com

In the last decade, the geometric filtering effect has been dealt with in a large number of scientific papers [5 - 14], which describe the conditions of occurrence for this effect, the filtering characteristics and the influence of this effect upon the vibrations behaviour of the railway vehicle.

This paper examines the influence of the geometric filtering effect on the ride comfort of the railway vehicles. Ride comfort is one of the criteria for evaluating the dynamic behaviour of the railway vehicles [16]. This is used to describe the degree of the passengers' comfort from the perspective of mechanical vibrations, taking into account the physiological characteristics of the human body [3]. The analysis stands on the results from numerical simulations developed on the basis of a theoretical model of rigid-flexible coupled type railway vehicle, which allows considering the vertical vibrations modes of the vehicle, relevant for the ride comfort – the carbody bounce, pitch and bending.

The paper is further structured into five sections. The first one introduces the vehicle model and the motion equations, the second one describes the calculation methodology for the ride comfort index according to EN 12299 standard [17] and UIC 513R leaflet [18], used in the paper to assess the ride comfort. A third section follows, with a synthetic description of the mechanism of geometric filtering occurrence and analysis of the efficiency of the geometric filtering effect at the resonance frequencies of the vibration modes of the vehicle carbody, depending on the geometric filtering velocities range. The section on results and discussions deals with the influence of the geometric filtering effect upon the dynamic response of the vehicle carbody, expressed as the power spectral density of the carbody vertical acceleration, and upon the ride comfort in three carbody reference points. These points, located at the carbody centre and against the two bogies, are considered critical points in terms of the ride comfort [19, 20].

2. The railway vehicle model

To study the geometric filtering effect upon the ride comfort at the vertical vibrations, the railway vehicle is reduced to a mechanical model equivalent of rigid-flexible coupled type (see figure 1) [13]. The two bogies and the corresponding wheelsets are modelled by rigid bodies. For the carbody, a 'flexible carbody' type model is adopted, where the carbody is represented by an Euler-Bernoulli beam equivalent. This model allows to consider the vibration modes of the vehicle in the vertical plane that are relevant for the ride comfort, namely the carbody rigid vibration modes (bounce z_c and pitch θ_c) and of the bogies' (bounce $z_{b1,2}$ and pitch $\theta_{b1,2}$) and the first vertical bending mode of the carbody.

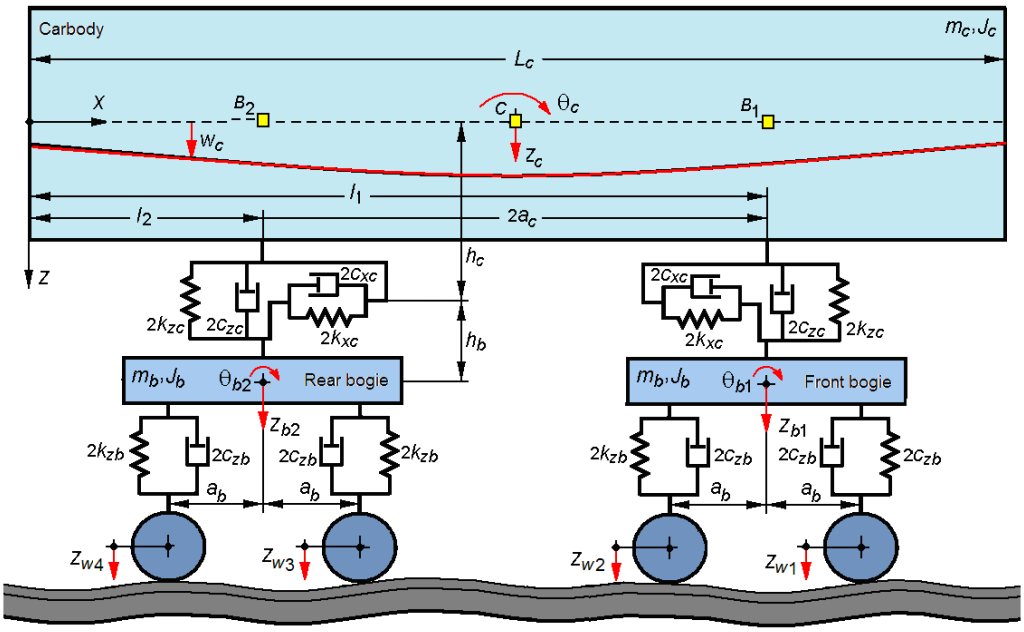

Fig. 1. The model of the railway vehicle.

Each wheelset is connected to the bogie frame with a Kelvin-Voigt system that models the primary suspension. The bogie is linked to the carbody through the secondary suspension modelled via a ensemble comprising two Kelvin-Voigt systems. The Kelvin-Voigt system for translation on the vertical direction models the elements themselves of the secondary suspension, while the Kelvin-Voigt system for translation on the longitudinal direction models the transmission system of the longitudinal forces between the carbody and the bogie. The secondary suspension plane finds itself at distance h_c from the carbody medium fiber and at distance h_b from the bogie centre of gravity.

The parameters of the model vehicle are shown in table 1.

As for the track model, the rigid track hypothesis is being used. The vertical track irregularities are leading to vertical displacements of the wheelsets, noted with $z_{w1...4}$. The vertical displacements of the four wheelsets $z_{w1...4}$ equals the vertical track irregularity as follows:

$$z_{w1,2} = \eta(x + a_c \pm a_b), \; z_{w3,4} = \eta(x - a_c \pm a_b), \tag{1}$$

where $\eta(x)$ is the function of the vertical track irregularity and $x = Vt$ is the coordinate for the carbody centre.

Table 1

The parameters of the vehicle model.

The parameters of the carbody and bogie			
Carbody mass	$m_c = 34.0 \cdot 10^3$ kg	Carbody length	$L_c = 26$ m
Bogie suspended mass	$m_b = 3.20 \cdot 10^3$ kg	Carbody wheelbase	$2a_c = 19.0$ m
Carbody inertia moment	$J_c = 1.96 \cdot 10^6$ kg·m^2	Bogie wheelbase	$2a_b = 2.56$ m
Bogie inertia moment	$J_b = 2.05 \cdot 10^3$ kg·m^2	Distances of the secondary suspension plane	$h_c = 1.30$ m
Bending modulus	$EI = 3.02 \cdot 10^9$Nm^2		$h_b = 0.20$ m
The parameters of the secondary suspension per bogie			
Vertical damping	$2c_{zc} = 34.3$ kNs/m	Vertical stiffness	$2k_{zc} = 1.2$ MN/m
Longitudinal damping	$2c_{xc} = 50.0$ kNs/m	Longitudinal stiffness	$2k_{xc} = 4.00$ MN/m
The parameters of the primary suspension per wheelset			
Vertical damping	$2c_{zb} = 26.1$ kNs/m	Vertical stiffness	$2k_{zb} = 2.2$ MN/m

It is considered that the track vertical irregularities can be represented as a stationary stochastic process, which can be described via the power spectral density [17]

$$S(\Omega) = \frac{A\Omega_c^2}{(\Omega^2 + \Omega_r^2)(\Omega^2 + \Omega_c^2)}, \tag{2}$$

where Ω is the wavenumber, $\Omega_c = 0.8246$ rad/m, $\Omega_r = 0.0206$ rad/m, and A is a coefficient depending on the track quality ($A = 4.032 \cdot 10^{-7}$ radm for a high level quality track, and $A = 1.080 \cdot 10^{-6}$ radm for a low level quality).

As a function of the angular frequency $\omega = V\Omega$, where V is the vehicle velocity, the power spectral density of the track irregularities is

$$G(\omega) = \frac{S(\omega/V)}{V} = \frac{A\Omega_c^2 V^3}{[\omega^2 + (V\Omega_c)^2][\omega^2 + (V\Omega_r)^2]}. \tag{3}$$

The motion equation of the carbody vehicle has the general form

$$EI\frac{\partial^4 w_c(x,t)}{\partial x^4} + \mu I\frac{\partial^5 w_c(x,t)}{\partial x^4 \partial t} + \rho_c\frac{\partial^2 w_c(x,t)}{\partial t^2} = \\ = \sum_{i=1}^{2} F_{zci}\delta(x - l_i) - h_c\sum_{i=1}^{2} F_{xci}\frac{\mathrm{d}\delta(x - l_i)}{\mathrm{d}x}, \tag{4}$$

where E is longitudinal modulus of elasticity, I - inertia moment of the beam's transversal section), μ - structural damping coefficient, and $\rho_c = m_c/L_c$ – beam mass per unit length; $\delta(.)$ is Dirac's delta function; distances $l_{1,2} = L_c/2 \pm a_c$ fix the supporting points position of the carbody on the secondary suspension. $F_{zc1.2}$ and $F_{xc1.2}$ represent the forces due to the secondary suspension,

$$F_{zc1,2} = -2c_{zc}\left(\frac{\partial w_c(l_{1,2},t)}{\partial t} - \dot{z}_{b1,2}\right) - 2k_{zc}\left[w_c(l_{1,2},t) - z_{b1,2}\right] \tag{5}$$

$$F_{xc1,2} = 2c_{xc}\left(h_c\frac{\partial^2 w_c(l_{1,2},t)}{\partial x \partial t} + h_b\dot{\theta}_{b1,2}\right) + 2k_{xc}\left(h_c\frac{\partial w_c(l_{1,2},t)}{\partial x} + h_b\theta_{b1,2}\right). \tag{6}$$

The vertical displacement of the carbody medium fiber w_c is the result of having the three vibration modes overlapped – bounce, pitch and vertical bending,

$$w_c(x,t) = z_c(t) + (x - L_c/2)\theta_c(t) + X_c(x)T_c(t), \tag{7}$$

where $T_c(t)$ is the coordinate of the carbody bending and $X_c(x)$ represents the natural function of this vibration mode, described in the equation

$$X_c(x) = \sin\beta x + \sinh\beta x - \frac{(\sin\beta L_c - \sinh\beta L_c)(\cos\beta x + \cosh\beta x)}{\cos\beta L_c - \cosh\beta L_c}, \tag{8}$$

with $\beta = \sqrt[4]{\omega_c^2\rho_c/(EI)}$, $\cos\beta L_c \cosh\beta L_c = 1$, (9)

where ω_c is the natural pulsation of the carbody bending.

The application of the modal analysis help infer the bounce, pitch and vertical bending equations,

$$m_c\ddot{z}_c = \sum_{i=1}^{2} F_{zci}, \tag{10}$$

$$J_c\ddot{\theta}_c = \sum_{i=1}^{2} F_{zci}\left(l_i - \frac{L_c}{2}\right) + \sum_{i=1}^{2} h_c F_{xci} \tag{11}$$

$$m_{mc}\ddot{T}_c + c_{mc}\dot{T}_c + k_{mc}T_c = \sum_{i=1}^{2} F_{zci}X_c(l_i) - \sum_{i=1}^{2} h_c F_{xci}\frac{\mathrm{d}X_c(l_i)}{\mathrm{d}x}. \tag{12}$$

where k_{mc} is the carbody modal stiffness, c_{mc} - carbody modal damping and m_{mc} - carbody modal mass.

The equations of bounce and pitch motions of the bogies are

$$m_b\ddot{z}_{b1} = \sum_{i=1}^{2} F_{zbi} - F_{zc1},\ m_b\ddot{z}_{b2} = \sum_{i=3}^{4} F_{zbi} - F_{zc2}, \tag{13}$$

$$J_b\ddot{\theta}_{b1} = a_b\sum_{i=1}^{2} \pm F_{zbi} - h_b F_{xc1},\ J_b\ddot{\theta}_{b2} = a_b\sum_{i=3}^{4} \pm F_{zbi} - h_b F_{xc2}, \tag{14}$$

where $F_{zb1...4}$ represent the forces due to the primary suspension,

$$F_{zb1,2} = -2c_{zb}(\dot{z}_{b1} + a_b\dot{\theta}_{b1} - \dot{z}_{w1,2}) - 2k_{zb}(z_{b1} + a_b\theta_{b1} - z_{w1,2}), \tag{15}$$

$$F_{zb3,4} = -2c_{zb}(\dot{z}_{b2} - a_b\dot{\theta}_{b2} - \dot{z}_{w3,4}) - 2k_{zb}(z_{b2} - a_b\theta_{b2} - z_{w3,4}). \tag{16}$$

The motion equations for the carbody and bogies make up a 7-equation system with ordinary derivatives. The system can be matrix-like written

$$\mathbf{M}\ddot{\mathbf{p}} + \mathbf{C}\dot{\mathbf{p}} + \mathbf{K}\mathbf{p} = \mathbf{P}\dot{z}_w + \mathbf{R}z_w, \tag{17}$$

where **M**, **C** and **K** are the inertia, damping and stiffness matrices, **P** and **R** are the displacement and velocity input matrices, and z_w is the vector of the heterogeneous terms.

3. Calculation of the ride comfort index at vertical vibrations

According to the standard of railway applications EN 12299 [17] and the UIC 513R leaflet [18], the cuantification of the comfort to vibrations is performed with ride comfort index ride comfort index (N_{MV}), and with a conventional scale linking the values of this index and the comfort sensation (see table 2).

Table 2

The significance of the ride comfort index N_{MV}.

Ride comfort index N_{MV}	Significance
$N_{MV} < 1$	Very comfortable
$1 \le N_{MV} < 2$	Comfortable
$2 \le N_{MV} < 4$	Medium
$4 \le N_{MV} < 5$	Uncomfortable
$N_{MV} \ge 5$	Very uncomfortable

The ride comfort index is calculated with the general relation [17, 18]

$$N_{MV} = 6 \cdot \sqrt{\left(a_{X95}^{Wad}\right)^2 + \left(a_{Y95}^{Wad}\right)^2 + \left(a_{Z95}^{Wab}\right)^2}, \tag{18}$$

where a_X, a_Y and a_Z is the root mean square of the longitudinal, lateral and vertical carbody acceleration, 95 refers to the quantile of order 95%, and W_{ad}, W_{ab} represent the weighting filters of the longitudinal, lateral, respectively vertical acceleration.

To evaluate the ride comfort for vertical vibrations, a partial ride comfort index is used, defined as in the general relation [17]

$$N_{MVZ} = 6a_{95}^{W_{ab}}, \tag{19}$$

where $W_{ab} = W_a \cdot W_b$ represents the weighting filter of the vertical acceleration.

The filter W_a is a passband filter with the following frequency weighting function

$$H_a(s) = \frac{s^2\left(2\pi f_2\right)^2}{\left[s^2 + \frac{2\pi f_1}{Q_{1`}}s + \left(2\pi f_1\right)^2\right]\left[s^2 + \frac{2\pi f_2}{Q_1}s + \left(2\pi f_2\right)^2\right]}, \tag{20}$$

where $s = i\omega$ (with $i^2 = -1$), $f_1 = 0.4$ Hz, $f_2 = 100$ Hz and $Q_1 = 0.71$.

The filter W_b takes into account the high human sensitivity to the vertical vibrations and has the frequency weighting function in the form of

$$H_b(s) = \frac{\left(s + 2\pi f_3\right) \cdot \left[s^2 + \frac{2\pi f_5}{Q_3} s + \left(2\pi f_5\right)^2 \right] 2\pi K f_4^2 f_6^2}{\left[s^2 + \frac{2\pi f_4}{Q_2} s + \left(2\pi f_4\right)^2 \right] \left[s^2 + \frac{2\pi f_6}{Q_4} s + \left(2\pi f_6\right)^2 \right] f_3 f_5^2} \tag{21}$$

where f_3 = 16 Hz, f_4 = 16 Hz, f_5 = 2.5 Hz, f_6 = 4 Hz, Q_2 = 0.63, Q_4 = 0.8 and K = 0.4.

Figure 2 shows the frequency weighting functions of the weighting filters W_a and W_b, whereas the figure 3 showcases the frequency weighting function $H_{ab} = H_a \cdot H_b$ of the filter W_{ab}. The latter shows that the mean comfort takes into account the higher sensitivity of the human body to vertical vibrations within the frequency interval of 4 Hz and 16 Hz.

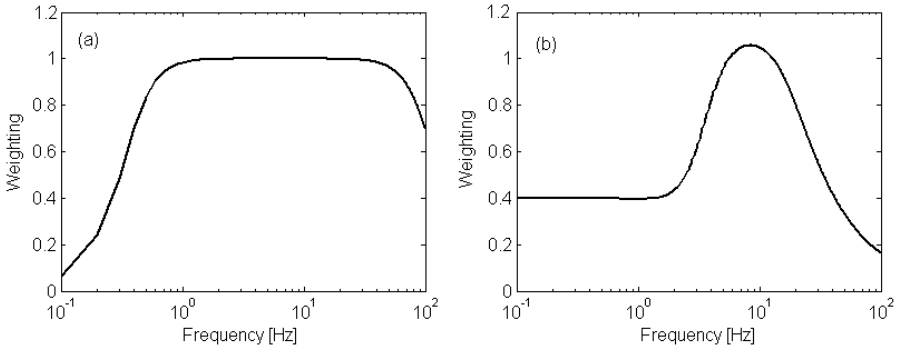

Fig. 2. The frequency weighting functions: (a) of the filter W_a; (b) of the filter W_b.

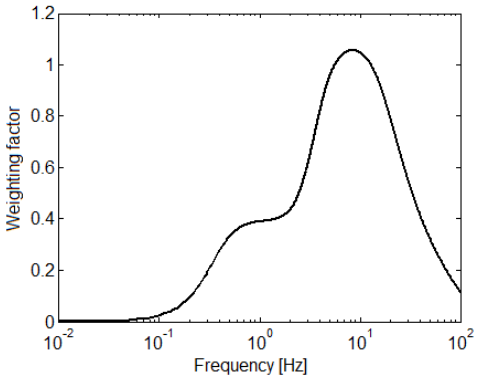

Fig. 3. The frequency weighting function of the filter W_{ab}.

As for the ride comfort, three carbody reference points are important, considered critical points [19, 20]. These points are marked in figure 1: C is

located at the carbody centre and B_1 and B_2 above the bogies, against the carbody leaning points on the secondary suspension.

The root mean square of vertical acceleration of the carbody reference points is calculated on the basis of the power spectral density of the carbody vertical acceleration, defined as follows

$$G_C(\omega) = G(\omega)[\overline{H}_C(\omega)]^2 = G(\omega)\omega^4\left[\overline{H}_{zc}(\omega) + X_c\left(L_c/2\right)\overline{H}_{T_c}(\omega)\right]^2, \tag{22}$$

$$G_{B_{1,2}}(\omega) = G(\omega)[\overline{H}_{B_{1,2}}(\omega)]^2 = G(\omega)\omega^4\left[\overline{H}_{z_c}(\omega) \pm a_c\overline{H}_{\theta_c}(\omega) + X_c(l_{1,2})\overline{H}_{T_c}(\omega)\right]^2 \tag{23}$$

where $\overline{H}_C(\omega)$ and $\overline{H}_{B_{1,2}}(\omega)$ stand for the response functions of the vertical acceleration of the carbody reference points, calculated in dependence on the frequency response functions corresponding to the rigid vibration modes of bounce and pitch $\overline{H}_{z_c}(\omega)$, $\overline{H}_{\theta_c}(\omega)$, and to the vertical bending $\overline{H}_{T_c}(\omega)$; $G(\omega)$ is the power spectral density of the vertical track irregularities (see eq. 2).

The root mean square of vertical acceleration is calculated as below

$$a_C = \sqrt{\frac{1}{\pi}\int G_C(\omega)\mathrm{d}\omega}, \tag{24}$$

$$a_{B_{1,2}} = \sqrt{\frac{1}{\pi}\int G_{B_{1,2}}(\omega)\mathrm{d}\omega}. \tag{25}$$

When adopting the hypothesis that the vertical accelerations have a Gaussian distribution with the null mean value, we will have the following relation to calculate the partial ride comfort index in the carbody reference points

$$N_{MV_C} = 6\Phi^{-1}(0.95)\sqrt{\frac{1}{\pi}\int_{0.5}^{10} G_C(\omega)\left|H_{ab}(\omega)\right|^2\mathrm{d}\omega}, \tag{26}$$

$$N_{MV_{B_{1,2}}} = 6\Phi^{-1}(0.95)\sqrt{\frac{1}{\pi}\int_{0.5}^{20} G_{B_{1,2}}(\omega)\left|H_{ab}(\omega)\right|^2\mathrm{d}\omega} \tag{27}$$

where $\Phi^{-1}(0.95)$ represents the quantile of the standard Gaussian distribution with the probability of 95%, and $H_{ab}(\omega) = H_a(\omega)\cdot H_b(\omega)$.

4. The geometric filtering effect

The geometric filtering effect is an important feature of the behaviour of vertical vibrations of the railway vehicles. The mechanism of generating the geometric filtering relies on the movements of the wheelsets' planes coming from the excitations resulting from the track. The vertical track irregularities are

transmitted to the wheelsets, thus producing vertical motions of bounce and pitch of their planes (fig. 4).

Under certain conditions, based on geometrical considerations, the plane of the wheelset of a bogie can only have pitch motions, as the bounce motion is not transmitted to the bogie frame – the plane of the wheelsets filters the bounce. Similarly, the plane of the wheelset can only have bounce motion, the pitch motion is not transmitted to the bogie, as the plane of the wheelsets filters the pitch.

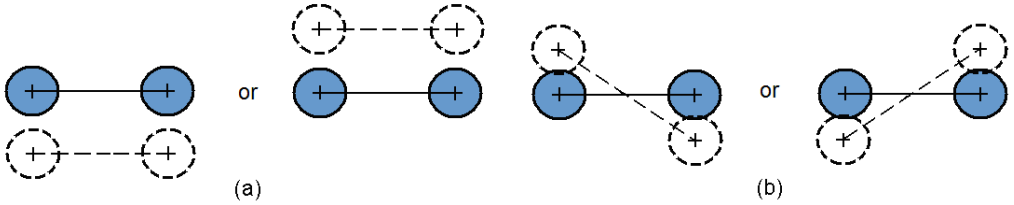

Fig. 4. The plane movements of the bogie wheelsets: (a) bounce; (b) pitch.

By combining the motions of bounce and pitch of the wheelsets planes of the two bogies, the symmetrical and asymmetrical motion modes of the planes of the vehicle wheelsets result, as shown in figures 5 and 6. For the symmetrical bounce of the vehicle wheelsets planes, all four vehicle wheelsets move in phase, whereas the wheelsets of a bogie are in anti-phase with the wheelsets of the other bogie for the antisymmetrical bounce of the wheelsets planes. The symmetrical pitch of the vehicle wheelsets planes is defined by rotations in anti-phase of the wheelsets' planes of the two bogies, while the anti-symmetrical pitch is described by in phase rotation motions of the wheelsets' planes [8, 12, 13].

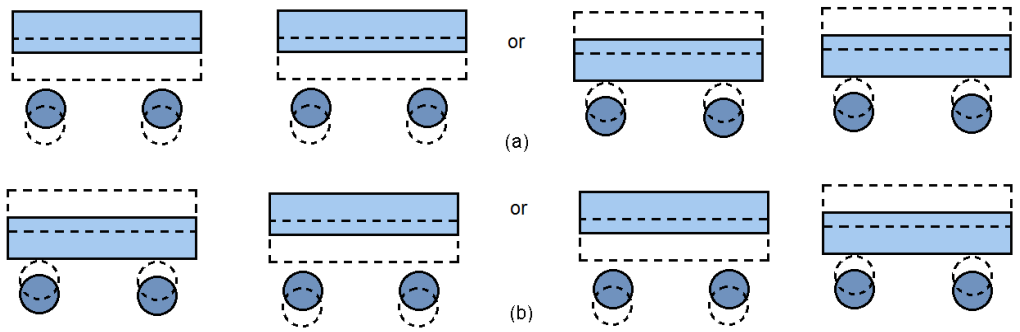

Fig. 5. The bounce of the vehicle wheelsets planes:
(a) symmetrical bounce; (b) antisymmetrical bounce.

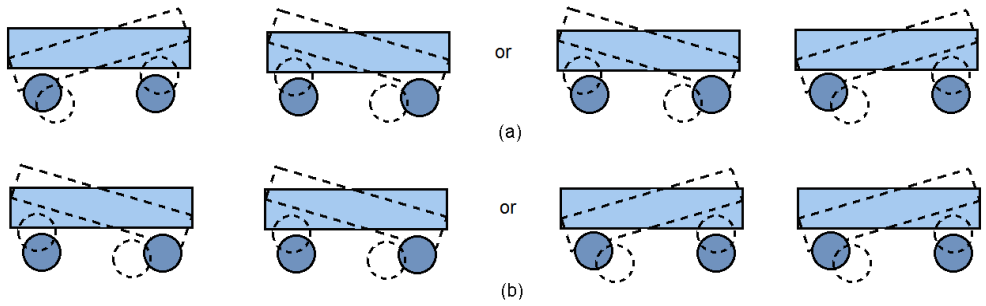

Fig. 6. The pitch of the vehicle wheelsets planes:
(a) symmetrical pitch; (b) anti-symmetrical pitch.

Practically, the geometric filtering effect is the result of the phase shift of the vertical motions of the wheelsets, generated by the track irregularities, where this shift comes from the distance between the vehicle wheelsets and velocity. This will provide the geometric filtering a selective character, depending on the bogie wheelbase, carbody wheelbase and velocity, hence a differentiated efficiency along the vehicle carbody and depending on the velocity.

The velocities corresponding to the geometric filtering effect depend on the bogie wheelbase or the carbody wheelbase and the excitation frequency $f = \omega/2\pi$ [14].

The symmetrical and antisymmetrical bounce of the wheelsets planes is filtered by the distance between the bogie wheelsets – the geometric filtering effect caused by the bogie wheelbase, at the velocities

$$V = \frac{4a_b f}{2n+1}, \text{ with } n = 0, 1, \ldots, \tag{28}$$

whereas the symmetrical and antisymmetrical pitch of the wheelsets planes is filtered by the bogie wheelbase at the velocities

$$V = \frac{2a_b f}{n}, \text{ with } n = 1, 2, \ldots. \tag{29}$$

The distance between bogies also filters the bounce and pitch motions of the wheelsets planes - filtering effect due to the carbody wheelbase. For the symmetrical bounce and the antisymmetrical pitch of the wheelsets planes, the geometric filtering effect is maximum at the velocities

$$V = \frac{4a_c f}{2n+1}, \text{ with } n = 0, 1, 2, \ldots, \tag{30}$$

and for the symmetrical bounce and antisymmetrical pitch of the wheelsets planes, at the velocities

$$V = \frac{2a_c f}{n}, \text{ with } n = 1, 2, \ldots \tag{31}$$

Figures 7 and 8 feature the filtering velocities at the resonance frequencies of the carbody bounce (1.17 Hz), carbody pitch (1.53 Hz) and carbody bending (8 Hz) calculated with relations (28) - (31), where $n_{max} = 15$.

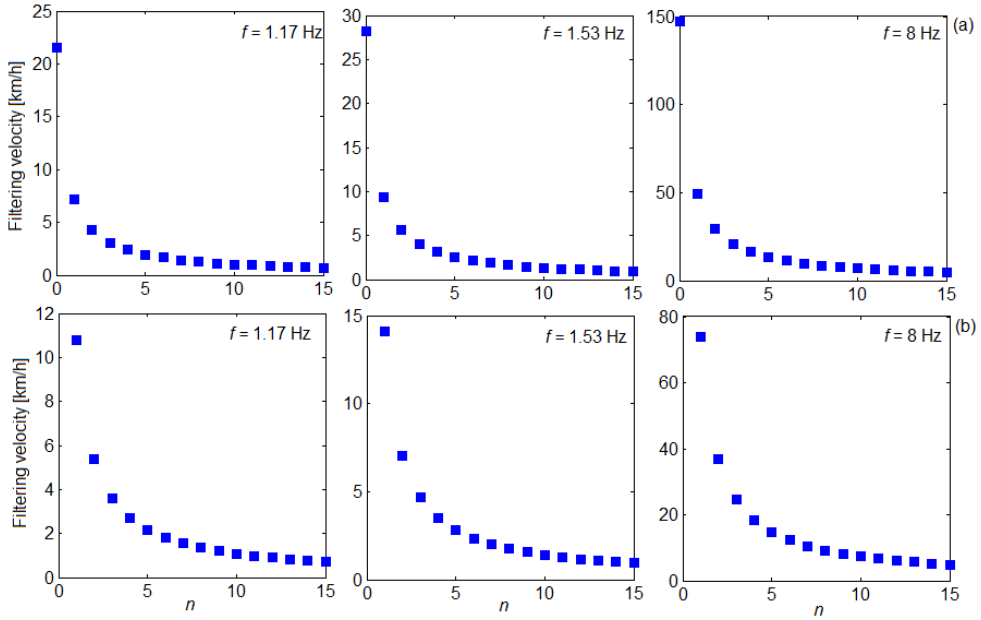

Fig. 7. Filtering velocities corresponding to the geometric filtering effect given by the bogie wheelbase (a) for the symmetrical and antisymmetrical bounce of the wheelsets planes; (b) for the symmetrical and antisymmetrical pitch of the wheelsets planes.

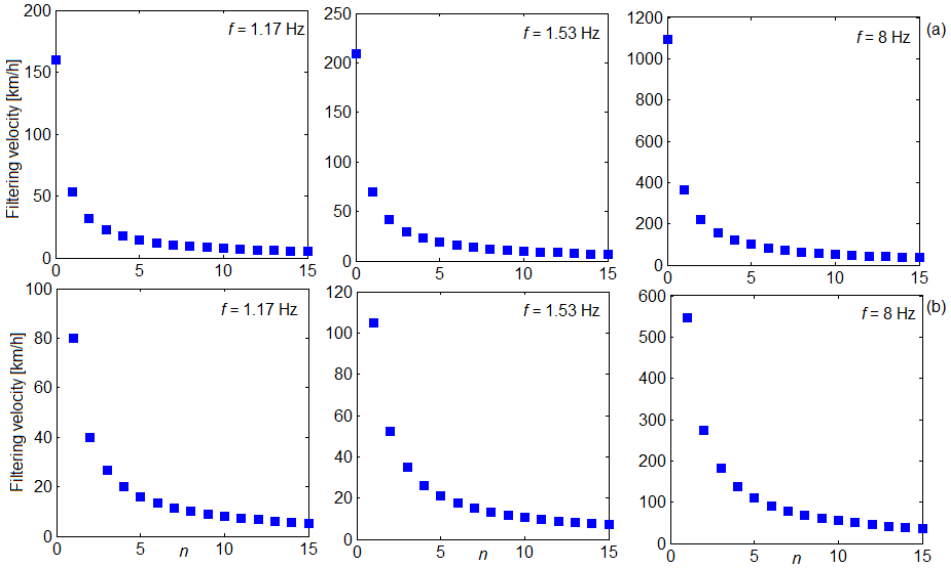

Fig. 8. Filtering velocities corresponding to the filtering effect given by the carbody wheelbase: (a) for the symmetrical bounce and antisymmetrical pitch of the wheelsets planes; (b) for the antisymmetrical bounce and the symmetrical pitch of the wheelsets planes.

The diagrams in figure 7 show that the bogie wheelbase generates a filtering effect at very low velocities, under 30 km/h, at the resonance frequencies of the carbody bounce and pitch. At the resonance frequency of the carbody bending, most filtering frequencies are in the range of low velocities, under 50 km/h, save for the maximum filtering velocity.

Based on the diagrams in figure 8, the range of the filtering velocities corresponding to the filtering effect due to the carbody wheelbase is analysed, excluding for this from the analysis the maximum filtering speeds. The filtering velocities of the symmetrical bounce and the antisymmetrical pitch of the wheelsets planes at the frequencies of 1.17 Hz and 1.46 Hz, do not exceed 55 km/h and 65 km/h, respectively. Similar observations can be made in relation to the filtering velocities of the antisymmetrical bounce and the symmetrical pitch in the wheelsets planes, namely filtering velocities being lower than 40 km/h and 50 km/h. Most of the filtering velocities are to be noticed to be in the range of very low values, under 20 km/h. As for the filtering velocities at the carbody bending frequency, they cover a large interval, spanning up to circa 365 km/h for the symmetrical bounce and antisymmetrical pitch of the wheelsets planes and 274 km/h for the antisymmetrical bounce and symmetrical pitch of the wheelsets planes. Nevertheless, most of the filtering velocities do not exceed 150 km/h.

The efficiency of the geometric filtering effect is assessed based on the velocity range covered by the filtering velocities. Summarizing of the above, the conclusion can be that the geometric filtering effect is efficient at only low and very low velocities, at the resonance frequencies of the vehicle carbody bounce and pitch. Likewise, the filtering velocities cover a large interval, including high running velocities, at the resonance frequency of the carbody bending.

5. Results and discussion

This section analyzes the results of the numerical simulations concerning the dynamic response of the vehicle carbody and the ride comfort in the carbody reference points, when running on a low quality track.

The diagrams in figure 9 present the dynamic response in the carbody reference points, expressed as the power spectral density of the vertical acceleration, for 20 - 250 km/h. At the carbody centre, the power spectral density of acceleration is dominated by the bounce vibrations (at 1.17 Hz). In the reference points located above the two bogies, the dominant vibration modes of the carbody are the pitch (at 1.53 Hz) and bounce. For high velocities, the peaks corresponding to the carbody bending can be also noticed in all reference points of the carbody (at 8 Hz). This vibration mode has a greater weight at the carbody centre [22, 23]. Along with the resonance frequency peaks of the carbody vibration modes, a series of minimum corresponding to the geometric filtering

effect can be seen. These values are more visible in figure 10, where the power spectral density of the vertical acceleration at the resonance frequencies of the carbody vibration modes is presented. It is observed that due to the geometric filtering effect, the behavior of vibrations of the carbody does not continually intensify with the increase in velocity.

The power spectral density of acceleration has a succession of maximum and minimum values; the maximum points correlate with the situation when the geometric filtering effect does not operate, while the minimum points show against the geometric filtering velocities. As above, the geometric filtering effect is more efficient at the resonance frequency of the carbody bending, in which case it covers a velocity range up to 200 km/h. Within this interval, most filtering velocities are found between 50 and 150 km/h.

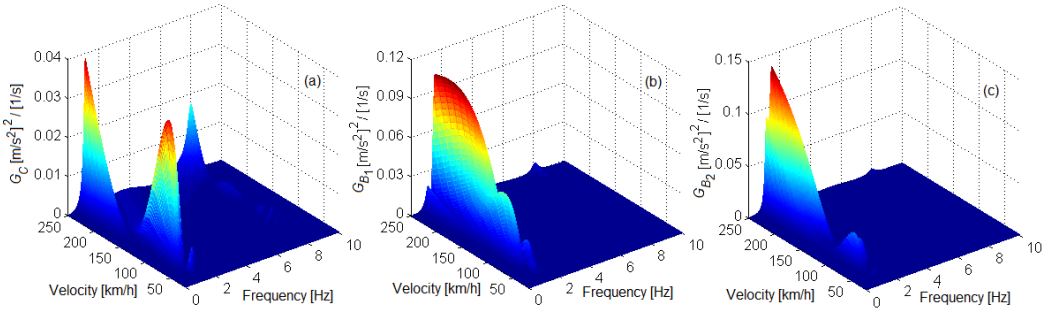

Fig. 9. Power spectral density of the carbody vertical acceleration:
(a) in point C; (b) in point B_1; (c) in point B_2.

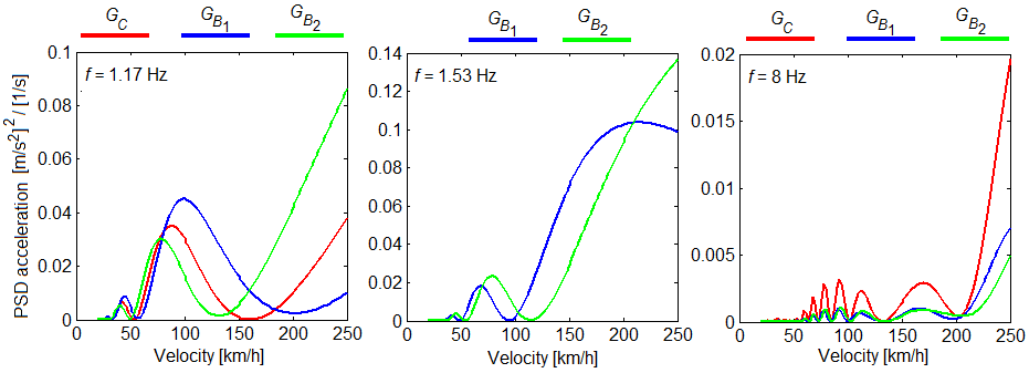

Fig. 10. Power spectral density of the carbody acceleration (PSD acceleration) at the resonance frequencies of the carbody vibration modes.

The increase in the carbody bending frequency in the 7 to 10 Hz interval leads to a reduction in the carbody flexibility by raising the bending modulus (EI) from $2.42 \cdot 10^9$ Nm^2 to $4.93 \cdot 10^9$ Nm^2 (see figure 11).

In this case, the velocity range covered by the geometric filtering velocities is expanded, thus increasing the efficiency of the filtering effect at high velocities. The diagrams in figure 11 show another important aspect, namely the reduction of the carbody bending vibrations by reducing the carbody flexibility.

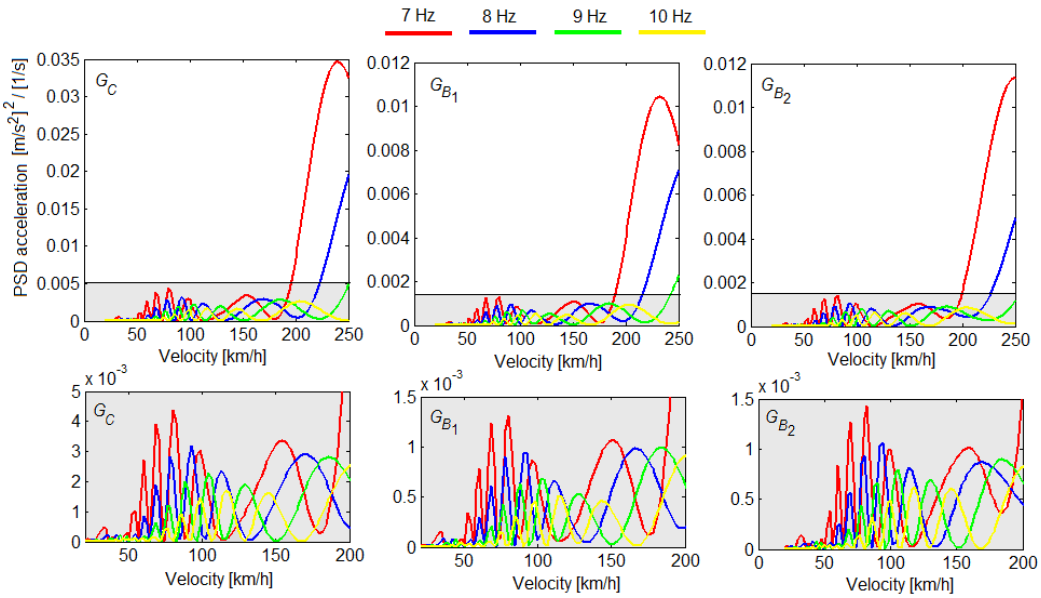

Fig. 11. Influence of the bending frequency on the power spectral density of the carbody acceleration.

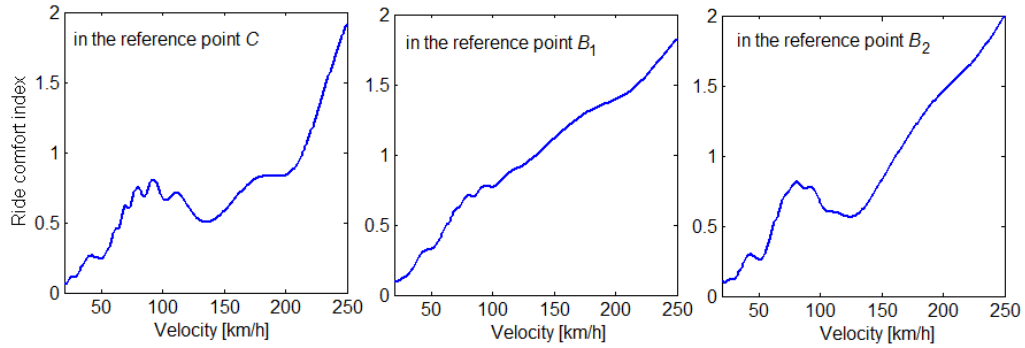

Fig. 12. Ride comfort index depending on the vehicle velocity.

Figure 12 shows the ride comfort indices in the carbody reference points calculated for velocities between 20 and 250 km/h. As a rule, the comfort index increases along with the velocity in all the carbody reference points. The increment of the comfort index is not continuous, however, due to the geometric filtering effect, which introduces a series of minimum values, velocity-dependent.

This effect is more visible up to velocity of 150 km/h. Regarding the values of the ride comfort indices in the carbody reference points, it is observed that they are very close up to the velocity of 80 km/h. As the velocity increases, the highest values of the comfort indices are recorded in the reference points above the two bogies. At high velocities, the comfort index at the carbody centre becomes comparable with the comfort indices in the points above the bogies. For instance, the comfort indices have the following values at 250 km/h - 1.91 – in point *C*, 1.82 – in point B_1, 1.86 – in point B_2.

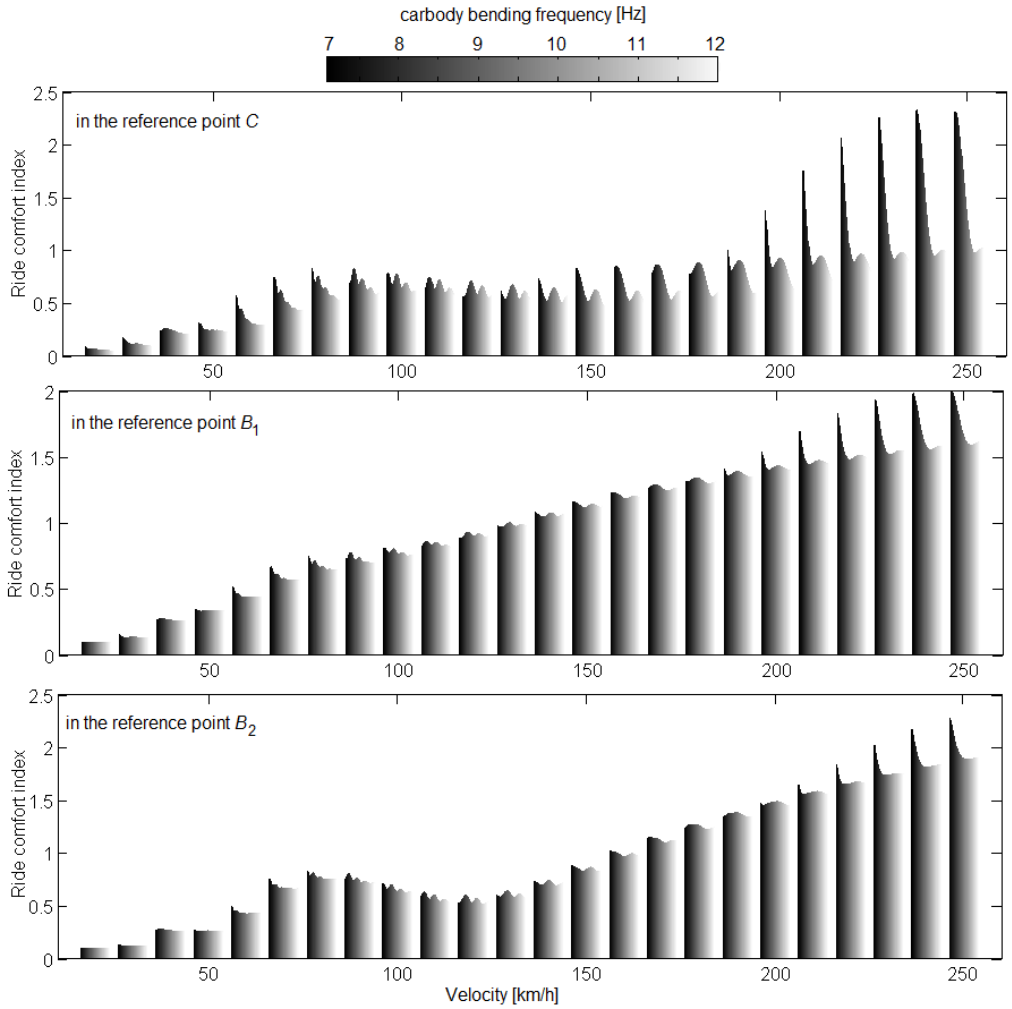

Fig. 13. Ride comfort index depending on the carbody bending frequency.

Based on the diagrams in figure 13, the influence of the geometric filtering effect upon the ride comfort index is analyzed, in correlation with the carbody bending frequency.

One observation is that the ride comfort index is affected by the increase in the carbody bending frequency in all the reference points, irrespective of velocity. Visible changes in the ride comfort index are nevertheless recorded at the carbody centre for high velocities, where the weight of the carbody bending vibrations is important (see figure 9, diagram (a)). As shown above, the geometric filtering velocities rise along with the carbody bending frequency (see figure 10). This is evident in the variation of the ride comfort index with the bending frequency, since the minimum values of the ride comfort index corresponding to the filtering velocities are moving in the sense of bending frequency increase.

6. Conclusions

The paper examines the influence of the geometric filtering effect of the excitations coming from the vertical track irregularities upon the dynamic response of the vehicle carbody and on the ride comfort. This analysis relies on the results from the numerical simulations concerning the power spectral density of the vertical acceleration of the vehicle carbody and ride comfort index in three important points of the carbody. The numerical simulation applications are developed on the basis of a theoretical model of the railway vehicle that takes into account the vertical vibration modes of the vehicle that are relevant for the ride comfort – the carbody bounce, pitch and bending.

The efficiency of the geometric filtering effect at the resonance frequencies of the vertical vibrations modes of the vehicle carbody is appreciated on the velocity range covered by the filtering velocities. At the resonance frequencies of the carbody bounce and pitch, the geometric filtering effect is only efficient at low and very low velocities. Instead, the filtering effect is efficient on a large velocity interval, which also covers the high velocities, at the resonance frequency of the carbody bending.

Due to the geometric filtering effect, the vibrations behaviour of the carbody does not intensify continually along with the velocity increase. This aspect is also emphasized for the ride comfort; the rise of the comfort index along with the velocity is not continuous due to the geometric filtering effect, which introduces a series of minimum values, velocity-dependent. For the flexible carbodies, the geometric filtering effect influences the ride comfort, mainly at velocities under 150 km/h. The velocity range extends itself through the reduction of the vehicle carbody flexibility. As for the efficiency of the geometric filtering effect in the carbody reference points, the geometric filtering has been confirmed to be more visible at the carbody centre, where the weight of the carbody bending vibrations is important.

Acknowledgments

The activity of Mihai Leu, PhD student, in this work has been funded by the European Social Fund from the Sectorial Operational Programme Human Capital 2014-2020, through the Financial Agreement with the title "Scholarships for entrepreneurial education among doctoral students and postdoctoral researchers (Be Entrepreneur!)", Contract no. 51680/09.07.2019 - SMIS code: 124539.

R E F E R E N C E S

[1]. *I. Sebeşan, T. Mazilu*, *Vibrations of the railway vehicles* (in Romanian), Ed. MatrixRom, Bucureşti, 2010.
[2]. *T. Mazilu, V.M. Dinu*, The vibration behaviour of a freight wagon in the presence of irregularities of the track, IOP Conf. Series: Materials Science and Engineering **vol. 682**, 2019, Article number 012007.
[3]. *S. Iwnicki*, Handbook of railway vehicle dynamics, Taylor & Francis Group, LLC, 2006.
[4]. *A. Orvanäs*, Methods for reducing vertical carbody vibrations of a rail vehicle, Report in Railway Technology Stockholm, KTH Engineering Sciences Department of Aeronautical and Vehicle Engineering, Division of Rail Vehicles, Sweden, 2010.
[4]. *J. Zhou, S. Wenjing*, Analysis on geometric filtering phenomenon and flexible car body resonant vibration of railway vehicles, Journal of Tongji University, **vol. 37**, issue 12, 2009, pp. 1653-1657.
[5]. *J. Zhou, R. Goodall, L. Ren, H. Zhang*, Influences of car body vertical flexibility on ride quality of passenger railway vehicles, Proceedings of the Institution of Mechanical Engineers, Part F: Journal of Rail and Rapid Transit, **vol. 223**, 2009, pp. 461-471.
[6]. *F. Cheli, R.Corradi*, On rail vehicle vibrations induced by track unevenness: Analysis of the excitation mechanism, Journal of Sound and Vibration, **vol. 330**, 2011, pp 3744–3765.
[7]. *M. Dumitriu*, Geometric filtering effect of vertical vibrations of railway vehicles, Analele Universităţii "Eftimie Murgu" Resiţa, **vol. 1**, 2012, pp. 48-61
[8]. *M. Dumitriu*, Influence of the suspension damping on ride comfort of passenger railway vehicles, UPB Scientific Bulletin, Series D: Mechanical Engineering, **vol. 74**, issue 4, 2012, pp. 75-90
[9]. *D. Gong, Y.J. Gu, Y. J. Song, J. Zhou*, Study on geometry filtering phenomenon and flexible car body resonant vibration of articulated trains, Advanced Materials Research, **vol. 787**, 2013, pp. 542-547.
[10]. *D. Gong, J. Zhou, W.J. Sun*, On the resonant vibration of a flexible railway car body and its suppression with a dynamic vibration absorber, Journal of Vibration and Control, **vol. 19**, issue 5, 2013, pp. 649-657
[11]. *M. Dumitriu*, Considerations on the geometric filtering effect of the bounce and pitch movements in railway vehicles, Annals of Faculty Engineering Hunedoara, **vol. 12**, issue 3, 2014, pp. 155-164.
[12]. *M. Dumitriu*, Analysis of the dynamic response in the railway vehicles to the track vertical irregularities. Part I: The theoretical model and the vehicle response functions, Journal of Engineering Science and Technology Review, **vol. 8**, 2015, pp. 24-31.
[13]. *M. Dumitriu*, Analysis of the dynamic response in the railway vehicles to the track vertical irregularities. Part II: The numerical analysis, Journal of Engineering Science and Technology Review, **vol. 8**, 4, 2015, pp. 32-39.

[14]. *Y.G. Kim, H.B. Kwon, S.W. Kim, C.K. Park, T.W. Park*, Correlation of ride comfort evaluation methods for railway vehicles, Proceedings of the Institution of Mechanical Engineers, Part F: Journal of Rail and Rapid Transit, **vol. 217**, 2003, pp. 73-88
[15]. *J. Wu, Y. Qiu*, Analysis of ride comfort of high-speed train based on a train-seat-human model in the vertical direction, Vehicle System Dynamics, Published online: 16 Jul 2020
[16]. EN 12299, Railway applications ride comfort for passengers measurement and evaluation, 1997.
[17]. UIC 513 R, Guidelines for evaluating passenger comfort in relation to vibration in railway vehicle, International Union of Railways, 1994.
[18]. *M. Dumitriu*, On the critical points of vertical vibration in a railway vehicle, Archive of Mechanical Engineering **vol. 61**, issue 4, 2014, pp. 115-140.
[19]. *D.I. Stănică, M. Dumitriu*, Critical points numerical analysis of ride comfort of the flexible railway carbody, IOP Conf. Series: Materials Science and Engineering, **vol. 682**, 2019, Article number 012007
[20]. C 116 Interaction between vehicles and track, RP 1, Power spectral density of track irregularities, Part 1: Definitions, conventions and available data, Utrecht, 1971
[21]. M. Dumitriu, A new approach to reducing the carbody vertical bending vibration of railway vehicles, Vehicle System Dynamics, **vol. 55**, 11, 2017, pp. 1787-1806.
[22]. *M. Dumitriu, C. Cruceanu*, Influences of carbody vertical flexibility on ride comfort of railway vehicles, Archive of Mechanical Engineering, **vol. 64**, issue 2, 2017, pp. 119-238.